

## Galvanomagnetic Properties of a Single-Crystal Sphere by the Induced-Torque Method. II. Magnetic Breakdown in Cadmium and Zinc

P. B. Visscher and L. M. Falicov

Department of Physics,\* University of California, Berkeley, California 94720

(Received 20 April 1970)

Experimental data from induced-torque measurements on cadmium and zinc for magnetic field directions perpendicular to the hexagonal axis are analyzed theoretically. In both Cd and Zn, magnetic breakdown between the first- and second-zone Fermi surfaces (the "caps" and the "monster") found by Datars and Cook is discussed. The change in topology, from open to closed orbits, makes the torque method an accurate tool for measuring the magnetic-breakdown parameters  $B_0$ ; these are 8.8 kG (for Cd,  $\vec{B}$  parallel to  $[10\bar{1}0]$ ), 18.7 kG (Cd;  $\vec{B}$  in  $[11\bar{2}0]$  direction), and 5.1 kG (Zn for  $\vec{B}$  along a direction in the basal plane  $7^\circ$  from  $[10\bar{1}0]$ ). For Zn, a second magnetic-breakdown phenomenon has been found. This is between the first-zone "caps" and the third-zone "needles," and produces a transition between closed orbits and a different kind of open orbits. The breakdown parameter for this second effect is 38.5 kG.

### I. INTRODUCTION

This paper is concerned with the application of the formula derived in the preceding paper<sup>1</sup> (referred to as I) to the analysis of some experimental results of Datars and Cook.<sup>2</sup> They measured the induced torque in cadmium and zinc due to open orbits present in both metals in which  $\vec{B}$  is perpendicular to the hexagonal axis. The geometry of their experiment is that described in I.

Magnetic-breakdown<sup>3</sup> effects on these orbits were found in the experiments.<sup>2</sup> As can be seen in Fig. 1, the torque increases at first as  $B^2$  (characteristic of open orbits) but then ( $\sim 5$  kG) it levels off and tends to saturation at higher fields (indicating closed orbits). This breakdown phenomenon is

well known<sup>4</sup> and takes place between the first- and second-band surfaces,<sup>5</sup> near the  $H$  point in the Brillouin zone. We have used a simple model for calculating the total conductivity (which we describe in Sec. II) and determined the value of the breakdown field (the parameter  $B_0$  such that the probability of breakdown in a magnetic field  $B$  is  $P = e^{-B_0/B}$ ) by least-squares fitting. In the data for zinc (Fig. 2,) after the initial quadratic rise and subsequent tendency towards saturation, the torque begins to rise again at very high fields ( $\sim 15$  kG). This suggests that the open orbits which close up at the first breakdown field are becoming open again. Such behavior can only occur if there is magnetic breakdown in the neighborhood of the  $K$  point in the Brillouin zone between the first-band

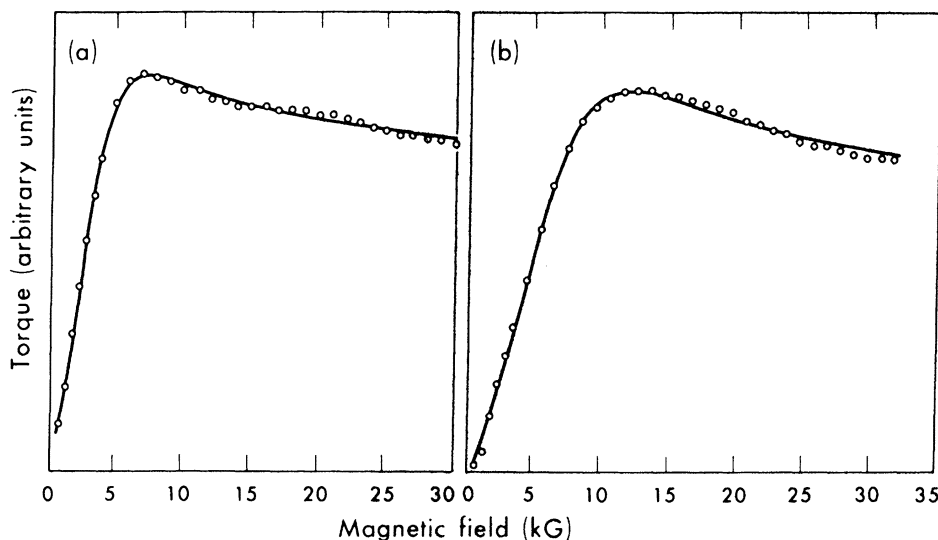


FIG. 1. Measured induced torque in cadmium as a function of  $B$ . Smooth curve is the best theoretical fit. (a)  $\vec{B}$  along  $[10\bar{1}0]$ ; fit with  $\tau = 1.57 \times 10^{-7}$  sec (assuming  $m^* = m$ , the free-electron mass). (b)  $\vec{B}$  along  $[11\bar{2}0]$ ,  $\tau = 1.22 \times 10^{-7}$  sec.

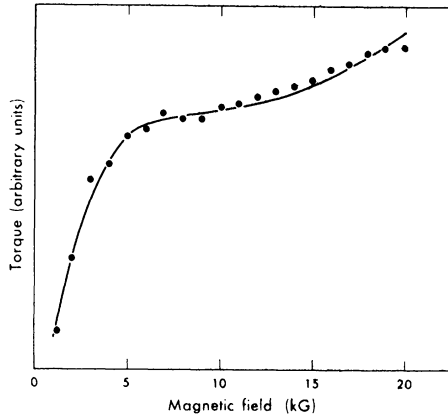


FIG. 2. Measured induced torque in zinc; smooth curve is best fit ( $\tau = 1.12 \times 10^{-7}$  sec).

“cap” hole surface and the third-band “needle” electron surface. We determined (again by least-squares fitting) the breakdown field  $B'_0$  at this point. This breakdown phenomenon has not, to our knowledge, been reported previously.

The results of the least-squares fitting and their interpretation are included in Sec. III.

## II. MODEL

The Fermi surfaces of cadmium and zinc<sup>5</sup> have only closed orbits for most field orientations. However, for fields in the hexagonal basal plane, there exists for each metal a small sheaf of open orbits all passing near the  $H$  point in the Brillouin zone and directed along the hexagonal axis. In the experiments of Ref. 2, the sample is mounted with the (0001) basal plane vertical, so the horizontal field  $\vec{B}$  may be swept through it. A rotation diagram (torque versus angle) is thus obtained. As  $\vec{B}$  passes through the basal plane there is a sharp peak in the torque coming from the open orbits. The height of this peak in the rotation diagram is plotted as a function of magnetic field strength  $B$ , and this is the curve we use in our discussions. By choosing various suspension axes in the (0001) plane, different open-orbit cross sections of the Fermi surface are obtained.

The conductivity at these open-orbit peaks is primarily due to that part of the Fermi surface which contains the open orbits, namely, a portion of the second-band “monster.” Therefore, our model treats these orbits in detail, as well as the first-band cap surfaces with which they may be connected by magnetic breakdown. The rest of the Fermi surface contains only closed orbits, and is taken into account through a free-electron-like contribution to the conductivity; this includes the

remainder of the monster (the “arms”) and the third-band electron lens.

The open-orbit part of the monster is approximated by a cylindrical surface; that is, all the open orbits are taken to be the same shape and obtainable from one another by rigid translation perpendicular to the cross-sectional planes (i. e., along  $\vec{B}$ ). Our model for the orbit shape is obtained by taking a cross section of the nearly-free-electron Fermi surface through the  $K$  point, perpendicular to  $\vec{B}$ . Thus the orbit is made up of arcs of circles, with different lengths and possibly different radii; it resembles quite closely the corresponding cross section of the actual monster surface of Cd or Zn. This may be done for each field direction in the basal plane; we have constructed the cross sections for  $B$  along  $[10\bar{1}0]$  and  $[11\bar{2}0]$ .

The result for  $[11\bar{2}0]$  is shown in Fig. 3(a) (the  $[10\bar{1}0]$  cross section is less simple, lacking the left-right mirror symmetry). The shape of the orbits at low fields (where there is no magnetic breakdown) is shown in Fig. 3(b); there is an open orbit from the second-band hole monster and a closed diamond-shaped orbit around the first-band hole cap. As the field is increased, breakdown occurs first at two points near the  $H$  point of the Brillouin zone [labeled 1 and 2 in Fig. 3(a)] in both Cd and Zn. As shown in Fig. 3(c), there results a single closed diamond-shaped orbit, similar in shape but larger than the low-field cap orbit in 3(b). The or-

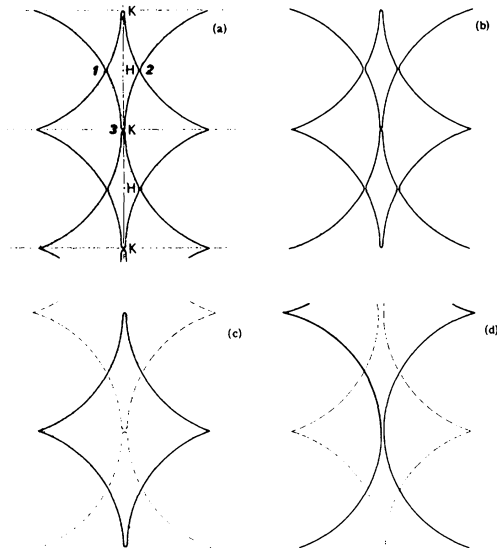


FIG. 3. (a) Model for  $[11\bar{2}0]$  cross section at Fermi surface in Cd or Zn. (b) Low-field orbits (no magnetic breakdown). (c) Intermediate field orbits [breakdown at points labeled 1 and 2 in (a)]. (d) High-field orbits (Zn only); breakdown also at point 3.

bits retain this shape at the highest fields investigated for Cd. For Zn, however, there is a further breakdown between the first-band caps and the third-band needle. The needle is a small pocket of electrons around the  $K$  point of the Brillouin zone, nestled between the tips of the cap and surrounded by the monster. It is not shown in Fig. 3, where the high-field open orbit in zinc [Fig. 3(d)] is depicted as jumping from the top of one cap directly to the bottom of the next. Because of the smallness of the needle, its effect on the conductivity is negligible; however, when magnetic breakdown couples it to the open orbits it becomes important because breakdown occurs across two gaps instead of one. An analysis of this situation<sup>3,6</sup> shows that the breakdown probability is given in this case by

$$P = \exp(-B'_0/B) [2 - \exp(-B'_0/B)]^{-1} \quad (2.1)$$

instead of the usual  $P = \exp(-B_0/B)$ . Thus the orbits in Zn at the highest fields are extremely free-electron-like with Bragg "reflections" occurring only in the monster, in the horizontal  $\Gamma KM$  plane of the Brillouin zone.

The calculation of the conductivity arising from the circular arcs depicted in Fig. 3(a) was made using the standard path-integral solution of the Boltzmann equation. The effects of magnetic breakdown on the connections between these arcs were taken into account in the manner described by Falicov and Sievert.<sup>6,7</sup>

The total conductivity is obtained by adding the contributions of all the cross sections, i. e., integrating over  $k_z$ ; in the case of our cylindrical model this involves just multiplying by the height in  $k$  space of the slab (cylinder). This factor, and the fact that there are two monster surfaces in each zone, is taken into account by an over-all scale factor  $\Sigma$  which we use as one of the fitting parameters.

In order to take into account the rest of the Fermi surface (the closed orbits), a conductivity correction term was added. It was of the form

$$\sigma_{\text{corr}} = \begin{pmatrix} A/(1+\omega^2\tau^2) & -D\omega\tau/(1+\omega^2\tau^2) & 0 \\ D\omega\tau/(1+\omega^2\tau^2) & C/(1+\omega^2\tau^2) & 0 \\ 0 & 0 & \sigma_0 \end{pmatrix}, \quad (2.2)$$

where

$$\omega = eB/mc \quad (2.3)$$

is the cyclotron frequency. This field dependence was chosen because it is the general form for the conductivity of an ellipsoidal Fermi surface.

The constants  $A$ ,  $C$ , and  $D$  are uniquely determined by requiring that the total conductivity  $\sigma$  be isotropic for  $\vec{B} = 0$  and that the  $B \rightarrow \infty$  limit of the

Hall conductivity correspond to a compensated metal, i. e.,

$$\sigma_{xy} = O(B^{-2}) \text{ as } B \rightarrow \infty. \quad (2.4)$$

The isotropy at zero field follows from the free-electron model (and is well satisfied by Cd and Zn).<sup>8</sup> The magnitude  $\sigma_0$  of this isotropic zero-field conductivity was used as a fitting parameter.

### III. COMPARISON WITH EXPERIMENTS

The least-squares fitting to the experimental data was done using as free parameters the scattering time  $\tau$  (assumed isotropic), the absolute magnitude scale for the torque (related to  $\Sigma$  and the radius of the sample), the zero-field conductivity  $\sigma_0$ , and the breakdown field  $B_0$ .

Figure 1 shows the best fits obtainable for the Cd curves for different field directions. The resulting breakdown fields were 8.8 kG  $[10\bar{1}0]$  and 18.7 kG  $[11\bar{2}0]$ . We are unable to explain this large difference; it does not seem possible that it could be due to anisotropy of the breakdown field, since breakdown occurs at all possible points for both field directions. Nor does it seem to be an experimental fluctuation; the curves for intermediate field directions<sup>2</sup> show the torque peak (hence the breakdown field) moving up continuously as the field turns from  $[10\bar{1}0]$  to  $[11\bar{2}0]$ . A similar though less pronounced effect seems to be present in Zn.

The analysis of Datars and Cook<sup>2</sup> used both a linear-chain model and the magnetoresistance calculated by Falicov and Sievert.<sup>6</sup> The least-squares fitting to the linear-chain model yielded breakdown fields of 7.0 kG at  $[10\bar{1}0]$  and 11.9 kG at  $[11\bar{2}0]$  which are approximately 40% lower than our values. The use of Falicov and Sievert's curves allowed for the possibility of different breakdown fields at points 1 and 2 of Fig. 3(a). The use of equal breakdown fields in this model gave a breakdown field of 8.7 kG at  $[10\bar{1}0]$  which is in excellent agreement with our value. This is reasonable because the present model of the first- and second-zones is an extension of the Falicov-Sievert model. To provide a better fit at low fields, Datars and Cook suggested a model with different breakdown fields at points 1 and 2, and for  $\vec{B}$  along  $[10\bar{1}0]$  obtained the best fit with a breakdown field of 10.8 kG. However, for  $\vec{B}$  along  $[11\bar{2}0]$ , 1 and 2 are equivalent. Even for  $\vec{B}$  along  $[10\bar{1}0]$ , where they are, in general, inequivalent, summing over all the cross-sectional planes perpendicular to  $\vec{B}$  moves points 1 and 2 around in such a way that for one cross section they become equivalent, and for others they approximately interchange positions in the Brillouin zone. For  $\vec{B}$  along  $[10\bar{1}0]$  a greatly improved fit with two fields might be regarded as evidence for anisotropy of breakdown field as the breakdown point moves

around the neck of the monster, though actual estimation of the highest and lowest values would require a more sophisticated model than ours. It seems likely, in fact, that differences in orbit shape from one cross section to another influence the conductivity more than differences in breakdown field.

We find that the fit improves somewhat when two fields are used (as it necessarily must when another variable parameter is introduced); the best fits are 5.2 and 10.2 kG for  $\vec{B}$  along  $[10\bar{1}0]$ , and 7.8 and 22.0 kG for  $\vec{B}$  along  $[11\bar{2}0]$ . But the decrease in the sum of the squares of the errors is so slight (less than 10% for  $[10\bar{1}0]$  and 20% for  $[11\bar{2}0]$ ) that it would be scarcely noticeable in Fig. 1. Thus we find that a single breakdown field is entirely adequate to explain the data.

Figure 2 shows the fit we obtain to Cook and Datar's induced-torque data for Zn,<sup>2</sup> for  $\vec{B}$  in the hexagonal basal plane  $7^\circ$  from  $[10\bar{1}0]$  direction. The parameters we vary are the same as for Cd, except that we now also allow breakdown at the  $K$  point, number 3 in Fig. 3(a). The breakdown field  $B'_0$  at this point is much higher than that at points 1 and 2 ( $B_0$ ), so at fields below about 10 kG the orbits (and hence the torque in Fig. 2) resemble those in Cd. After breakdown occurs at point 3, the orbits become open again [Fig. 3(d)] so the induced torque begins to rise quadratically in the manner characteristic of open orbits (see I).

To fit the data for Zn we used the same model for the orbits as for Cd (Fig. 3); the Fermi surfaces of these metals are quite similar in general form.<sup>9</sup> The only difference is, as mentioned above, the breakdown at point 3. The least-squares fitting yielded for the breakdown parameters

$$B_0 = 5.1 \text{ kG}$$

at points 1 and 2 (near  $H$  in the Brillouin zone in the actual structure) and

$$B'_0 = 38.5 \text{ kG}$$

for point 3 (at  $K$  in the actual structure).

The values reported here have an estimated error of about 20%. The magnetic-breakdown phenomenon near  $H$  has been studied before, but the values of  $B_0$  could not be accurately determined. Tsui and Stark<sup>4</sup> point out that in Cd the orbit  $\gamma'$  (their notation), which involves breakdown close to  $H$ , could not be observed for fields less than 32 kG, while Grassie<sup>10</sup> could only bracket the value of  $B_0$  between 2 and 120 kG.

The situation for Zn seems to have been finally clarified. Stark<sup>11</sup> estimates  $B_0$  to be about 17 kG but states that the openness of the monster parallel to the hexagonal axis is not completely eliminated for magnetic field strengths as large as 70 kG. The statement seems paradoxical and the paradox is solved only if the second breakdown phenomenon here described takes place.

One remark is in order. As far as we are aware, this is the first time that magnetic breakdown has been found between two nonconsecutive bands. Breakdown between the caps (first band) and the needles (third band) implies tunneling across the second-band monster. Such a phenomenon is theoretically possible but had not previously been observed.

In conclusion we would like to point out that the advantages of the induced-torque method, which uniquely singles out the open-orbit contributions, are evident in the cases we have discussed here, and should also be demonstrated in many other cases, especially those involving compensated polyvalent metals.

#### ACKNOWLEDGMENT

The authors are grateful to Professor W. R. Datars for communicating his results prior to publication and for several stimulating discussions on the torque method in general and the Cd and Zn data in particular.

\*Work supported in part by the National Science Foundation under Grant No. GP13889.

<sup>1</sup>P. B. Visscher and L. M. Falicov, preceding paper, Phys. Rev. B 2, 1518 (1970).

<sup>2</sup>W. R. Datars and J. R. Cook, Phys. Rev. 187, 769 (1969); J. R. Cook and W. R. Datars (unpublished).

<sup>3</sup>R. W. Stark and L. M. Falicov, in *Progress in Low Temperature Physics*, Vol. V, edited by C. J. Gorter (North-Holland, Amsterdam, 1967), p. 235, and references therein.

<sup>4</sup>D. C. Tsui and R. W. Stark, Phys. Rev. Letters 16, 19 (1966).

<sup>5</sup>For the detailed description of the Fermi surfaces of Cd and Zn see R. W. Stark and L. M. Falicov, Phys. Rev. Letters 19, 795 (1967); R. C. Jones, R. G. Goodrich,

and L. M. Falicov, Phys. Rev. 174, 672 (1968); O. L. Steenhaut and R. G. Goodrich, *ibid.* B 1, 4511 (1970) and the many references therein.

<sup>6</sup>L. M. Falicov and P. R. Sievert, Phys. Rev. 138, A88 (1965).

<sup>7</sup>The only difference between our calculations and those of Ref. 6 is that we have not restricted ourselves to equal-length (isochronous) arcs.

<sup>8</sup>O. P. Katyal and A. N. Gerritsen, Phys. Rev. 178, 1037 (1968).

<sup>9</sup>The monster in Zn is multiply connected at the  $\Gamma$ KM plane. This connectivity is, however, irrelevant for the field directions discussed in this paper.

<sup>10</sup>A. D. C. Grassie, Phil. Mag. 9, 847 (1964).

<sup>11</sup>R. W. Stark, Phys. Rev. 135, 1698 (1964).